Contents lists available at ScienceDirect

Science of the Total Environment

Models of radon exhalation from building structures: General and case-specific solutions

C. Di Carlo *, A. Maiorana, M. Ampollini, S. Antignani, M. Caprio, C. Carpentieri, F. Bochicchio

Italian National Institute of Health / National Center for Radiation Protection and Computational Physics, Viale Regina Elena, 299, 00161 Rome, Italy

HIGHLIGHTS

- Four mathematical models account for radon transport and generation mechanisms.
- Case-specific boundary conditions represent the actual exhalation in buildings.
- Analytical solutions are developed to assess the radon exhalation in all conditions.
- The solutions provided serve as a tool to optimize the remedial action strategies.
- The work output may help to achieve the circular economy goals in building industry.

GRAPHICAL ABSTRACT
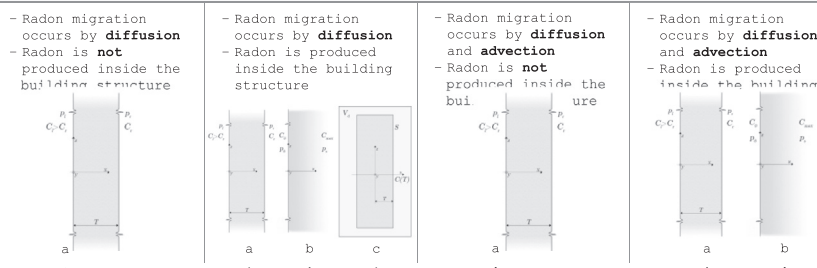
ARTICLE INFO

ABSTRACT

Assessing the radon activity that exhales from building structures is crucial to identify the best strategies to prevent radon from entering a building or reducing its concentration in the inhabited spaces. The direct measurement is extremely difficult, so the common approach has consisted in developing models describing the radon migration and exhalation phenomena for building porous materials. However, due to the mathematical complexity of comprehensively modelling the radon transport phenomenon in buildings, simplified equations have been mostly adopted until now to assess the radon exhalation. A systematic analysis of the models applicable to radon transport has been carried out and it has resulted in four models differing in the migration mechanisms – only diffusive or diffusive and advective – and the presence of inner radon generation. The general solutions have been obtained for all the models. Moreover, three case-specific sets of boundary conditions have been formulated to account for all the actual scenarios occurring in buildings: both perimetral and partition walls and building structures in direct contact with soil or embankments. The corresponding case-specific solutions obtained serve as a key practical tool to improve the accuracy in assessing the contribution of building materials to indoor radon concentration according to the site-specific installation conditions in addition to the material inner properties.

1. Introduction

The population exposure to indoor radon is the leading cause of lung cancer among non-smoker (United States Environmental Protection Agency, 2003; World Health Organization, 2009; IARC, 2012). The building materials are a well-recognized source of indoor radon (UNSCEAR, 2008). Many studies have specifically addressed the role of building materials in contributing to indoor radon concentration and extensive dataset are now available (e.g., (Trevisi et al., 2018)).

Current national and international regulations (e.g., (European Commission, 2014)) require to consider any source of radon including the building materials. Developing methods to identify building materials that largely contribute to the indoor radon concentration is crucial to choose the best preventive and remedial strategies to reduce the indoor exposure to radon (e.g., (Lucchetti et al., 2020; Lucchetti et al., 2022)). The

* Corresponding author.
E-mail address: christian.dicarlo@iss.it (C. Di Carlo).

United Nations Scientific Committee on Effects of Atomic Radiation (UNSCEAR, 2006) reported as significant sources of indoor radon materials that have a combination of elevated levels of 226Ra and porosity. The contribution of building materials to the indoor radon concentration, despite being generally low (UNSCEAR, 2000), under some circumstances may become significant or even predominant (Sabbarese et al., 2021; Denman et al., 2007; Barros-Dios et al., 2007), e.g., in dwellings located at floors higher than ground one (Yarmoshenko et al., 2022; Bochicchio et al., 1999), especially in newly built highly air tightened houses (McGrath et al., 2021), or in historic buildings with inner filler ultra-thick walls (Frutos et al., 2021).

The radon exhalation rate – the radon activity coming out of building structures per unit time and surface – depends on:

i) the material properties, i.e., radium content, diffusivity, emanation coefficient, porosity and permeability.
ii) The installation conditions, i.e., width and geometry of the slab, how units are laid in and bound together, binding elements and covering layers used.
iii) The environmental parameters that affect:

   a. the inner characteristics of the building materials, e.g., the emanation coefficient strongly depends on temperature (Tuccimei et al., 2009; Iskandar et al., 2004) and water content (Strong and Levins, 1982);
   b. the radon migration, e.g., the air exchange rate strongly influences the indoor radon concentration (Vasilyev et al., 2015; Collignan and Powaga, 2019), so the concentration gradient regulating the diffusive transport.

Some environmental parameters may affect both the material characteristics and the radon migration mechanism, e.g., the pressure gradient over the slab affects the air permeability (Chauhan and Kumar, 2015) and the advective transport itself.

According to the current state of knowledge and technology, reliable values of radon exhalation rate from building structure can be achieved by:

i) in-site measurement of radon exhalation rate directly from the wall surface (I.O.f. Standardization, Technical report, 2012);
ii) combination of measurement and mathematical modelling, i.e., the radon exhalation is measured from a building material sample (Ishimori et al., 2013) and the resulting rate is associated to the corresponding actual exhalation rate from building structure made of the same material (Sahoo et al., 2011; Orabi, 2018);
iii) mathematical modelling of the radon generation and migration in building structures and the resulting exhalation from the free surfaces (e.g., (López-Coto et al., 2014; Jonassen and McLaughlin, 1980)).

The formulations of the radon exhalation adopted by the ii) and iii) have been mostly obtained from a simplified model – only diffusive radon transport and not negligible inner radon generation – by considering case-specific boundary conditions, i.e., the wall is supposed to divide spaces with similar radon concentration such to assure the radon concentration function to be even. The actual scenarios occurring in buildings may significantly differ, so case-specific solutions should be considered to assure the reliability of the results: the radon transport model should consider all the migration mechanisms and a much wider sets of boundary conditions better-fitting the actual scenarios.

This work has reviewed and systematically organized the mathematical one-dimensional models applicable to radon generation and transport in building porous materials depending on the migration mechanisms and the presence of inner radon source, i.e. radium-226 atoms. The general solutions are developed for all the models considered and the corresponding specific solutions are obtained and reported for sets of boundary conditions that describe all the actual scenarios likely to occur in buildings. The equations for radon exhalation provided are a key practical tool to assess the actual building materials contribution to indoor radon concentration. Such a tool may play a role in the optimization of radon reduction strategies and in the achievement of the circular economy objectives in building material industry.

2. Materials and methods

The building structure exhaling radon is modelled as a slab of uniform thickness and homogeneous composition. The radon concentration inside the slab is assumed to vary only along the axis orthogonal to the exhaling surface so the corresponding radon flux is one-dimensional.

The models adopted in literature for radon migration within porous media have been reviewed and organized in four different formulations depending on the migration mechanisms and the presence of inner radon generation:

i. radon migrates by diffusion through the slab without inner radon generation;
ii. radon migrates by diffusion through the slab with inner radon generation;
iii. radon migrates by diffusion and advection through the slab without inner radon generation;
iv. radon migrates by diffusion and advection through the slab with inner radon generation.

Although thermo-diffusion was reported to be likely transport mechanism in some specific circumstances (Minkin, 2002), this work refers to the radon transport mechanisms presented and discussed in the latest UNSCEAR publications (UNSCEAR, 2006; UNSCEAR, 2000).

The assumption underlying all the four models is the negligibility of the material moisture content (Eq. (37) of Appendix A).

The advective transport is driven by the air absolute pressure difference over the building envelope, i.e., between the slab sides, and depends on the air permeability of the material (Eq. (45) in Appendix A). Some technical regulations on buildings require indoors to be maintained under negative pressure to avoid moisture condensation on building envelope likely to result in damaging it (Leivo et al., 2015; WHO, 2019). Furthermore, stack effect, wind effect, and natural ventilation usually establish an under pressure inside the building of the order of 5–10 Pa. This gradient generally increases during the heating season up to 15 Pa (Chauhan and Kumar, 2015) or if energy efficiency measures are applied in the building (Leivo et al., 2015).

Pertaining to the radon generation term, the radon source inside the material can be neglected when radium-226 concentration or emanation fraction is low (Eq. (38) in Appendix A): both circumstances reflect on the reduction of radon atoms available in pores for the migration. Some authors specifically addressed the negligibility of the source term in building materials (Rogers et al., 1995).

The general solution has been analytically developed for each model in steady-state, i.e., the radon concentration function within the slab keeps constant over the time.

Three case-specific sets of boundary conditions have been developed to represent all the actual scenarios, i.e., constructive features and values of environmental parameters, occurring in buildings:

a. fixed radon concentration on both sides of finite slab.
b. fixed radon concentration on a side of an infinite slab;
c. finite slab inside a vessel with unknown radon concentration inside.

The a. set accounts for both perimetral and partition walls in buildings, the b. one for floors directly attached to the ground or walls adjacent to embankments and the c. one for partition walls dividing spaces with similar radon concentrations. The specific analytical solutions have been developed from the general transport equations considering only the sets of boundary conditions applicable to the corresponding models: the combinations are reported in Table 1.

Table 1

Combination of transport models and boundary conditions for which analytical solution have been developed.

	Only diffusive transport		Diffusive and advective transport	
	Model	Boundary conditions	Model	Boundary conditions
No inner radon generation	i.	a.	iii.	a.
Inner radon generation	ii.	a. b. c.	iv.	a. b.

3. Results

3.1. Radon only diffusive transport through a slab without inner radon generation

In case of only diffusive radon transport along the x-axis and no radon generation in the slab, the radon concentration can be modelled as follows:

$$D_e \frac{d^2 C_{Rn}(x)}{dx^2} - \lambda_{Rn} C_{Rn}(x) = 0 \tag{1}$$

where:

− D_e is the effective diffusivity (Eq. (41) of Appendix A) of porous medium along the x-axis (m^2 s^{-1}),
− $C_{Rn}(x)$ is the activity concentration of radon per unit volume of interstitial space (Bq m^{-3}),
− λ_{Rn} is the radon decay constant (s^{-1}).

The solution of the homogeneous differential Eq. (1) is:

$$C_{Rn} = A e^{-\sqrt{\frac{\lambda_{Rn}\varepsilon}{D}} x} + B e^{\sqrt{\frac{\lambda_{Rn}\varepsilon}{D}} x} = A e^{-\frac{x}{R}} + B e^{\frac{x}{R}} = A e^{-xr} + B e^{xr} \tag{2}$$

being ε the material porosity, R the diffusion length and $r = \frac{1}{R}$ its inverse (Eqs. (42) and (43) of Appendix A). A and B are the integration constants depending on the boundary conditions.

3.1.1. Fixed radon concentration on both sides of a finite slab

Referring to Fig. 1, the boundary conditions can be written as follows:

$$\begin{cases} C_{Rn}(x=0) = C_l \\ C_{Rn}(x=T) = C_r \end{cases} \tag{3}$$

The absolute air pressures on the sides of the slab are the same, i.e., $p_l = p_r$. The resulting general solution of Eq. (2) is:

$$C_{Rn}(x) = \frac{1}{2\sinh(rT)} \left[\left(C_l e^{rT} - C_r \right) e^{-rx} + \left(C_r - C_l e^{-rT} \right) e^{rx} \right] \tag{4}$$

The radon concentration function is reported in Fig. 2 for different building materials.

The corresponding exhalation rate, E (Bq m^{-2} s^{-1}), on the right side of the slab can be computed as (Jonassen and McLaughlin, 1980):

$$E(T) = -D \frac{dC_{Rn}(x)}{dx}\bigg|_{x=T} = \frac{Dr}{2\sinh(rT)} \left[C_l - C_r \cosh(rT) \right] \tag{5}$$

If radon concentration on a side is supposed to be very low – e.g., perimetral walls separates the indoors from the outdoor air whose worldwide average radon concentration is of about 10 Bq m^{-3} (UNSCEAR, 1993) – Eqs. (4) and (5) turn into:

$$C_{Rn}(x) = \frac{C_l}{2\sinh(rT)} \left[\left(e^{rT} \right) e^{-rx} + \left(e^{-rT} \right) e^{rx} \right] \tag{6}$$
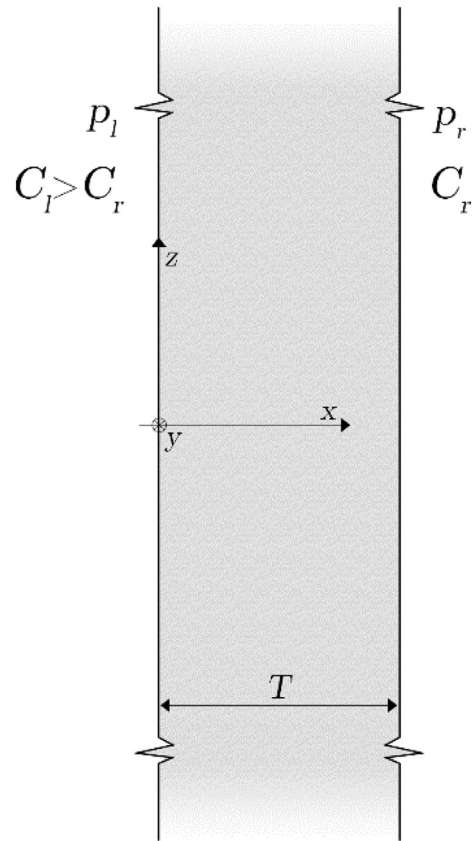
Fig. 1. Schematic representation of slab made of a porous material. The radon concentration on both sides of the wall is constant if steady-state is reached: C_l on the left and C_r on the right. Slab dimensions along y- and z-axes are much greater than along the x-axis. p_l and p_r are the absolute air pressures in the spaces on the left and the right side of the slab, respectively.

$$E(T) = -D \frac{dC_{Rn}(x)}{dx}\bigg|_{x=T} = \frac{D C_l}{\sinh(rT)} \tag{7}$$

Eqs. (6) and (7) are also applicable to partition structures separating premises with different radon concentration and to experimental set-up conceived to measure the diffusivity of building materials (Keller et al., 2001; Culot et al., 1976). Similar measurements requires a constant radon concentration on a side of the slab and recording the slow increase of radon level on the other side due to the only diffusive transport (e.g., (Hsu et al., 1994)).

3.2. Radon only diffusive transport through a slab with inner radon generation

If both the radium-226 concentration and the emanation fraction are not negligible, and the radon migration happens along the x-axis only by molecular diffusion, the concentration can be modelled as follows:

$$D_e \frac{d^2 C_{Rn}(x)}{dx^2} - \lambda_{Rn} C_{Rn}(x) + G_v = 0 \tag{8}$$

where G_v is the radon production rate per unit pore volume (Bq s^{-1} m^{-3}) computed according to Eq. (38) in Appendix A.

The resulting general solution of the inhomogeneous Eq. (8) is:

$$C_{Rn}(x) = A e^{-xr} + B e^{xr} + \frac{G_v}{\lambda_{Rn}} \tag{9}$$

being A and B the integration constants of the general solution and $\frac{G_v}{\lambda_{Rn}}$ the particular one of the inhomogeneous differential equation.
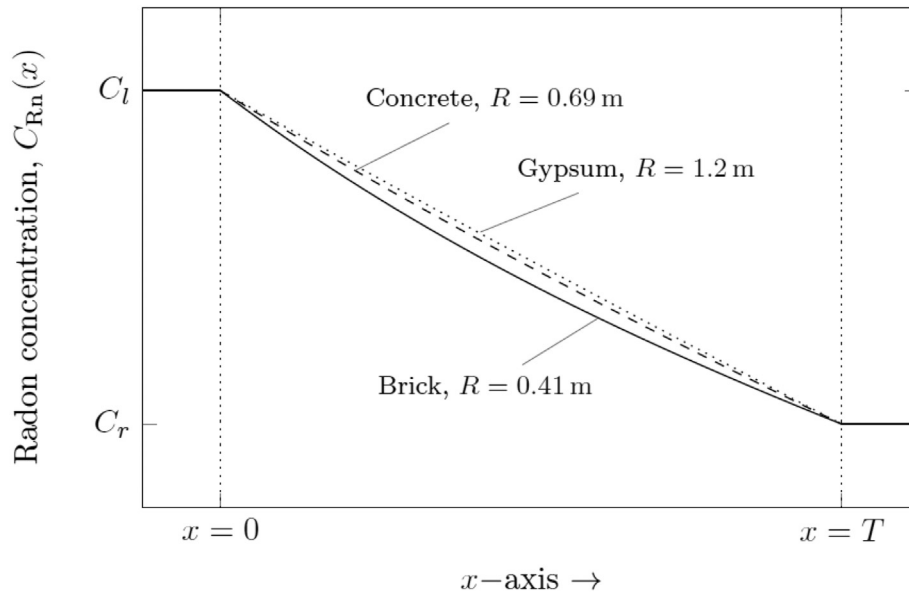
Fig. 2. Radon concentration function along the x-axis in steady-state for walls made of three different materials if the inner radon generation is negligible. Radon diffusion length of brick, aerated concrete and gypsum are taken from Keller, Hoffmann and Feigenspan (Keller et al., 2001).

3.2.1. Fixed concentrations on both sides of a finite slab

Referring to Fig. 1, the boundary conditions are the same already seen in Section 3.1.1 (Eq. (3)). The general solution for radon concentration results is obtained from Eq. (9):

$$C_{Rn}(x) = \frac{1}{2 \sinh (rT)} \left\{ \left(C_l e^{rT} - C_r \right) e^{-rx} + \left(C_r - C_l e^{-rT} \right) e^{rx} \right.$$

$$\left. + 2\frac{G_v}{\lambda_{Rn}} \left[\sinh \left(r(x-T) \right) - \sinh \left(rx \right) + \sinh \left(rT \right) \right] \right\} \qquad (10)$$

The radon concentration function is reported in Fig. 3 for different building materials.

The exhalation rate on the right side of the slab can be computed as:

$$E(T) = -D \frac{dC_{Rn}(x)}{dx}\bigg|_{x=T}$$

$$= -\frac{Dr}{\sinh(rT)} \left\{ -C_l + C_r \cosh(rT) + \frac{G_v}{\lambda_{Rn}} [1 - \cosh(rT)] \right\} \qquad (11)$$
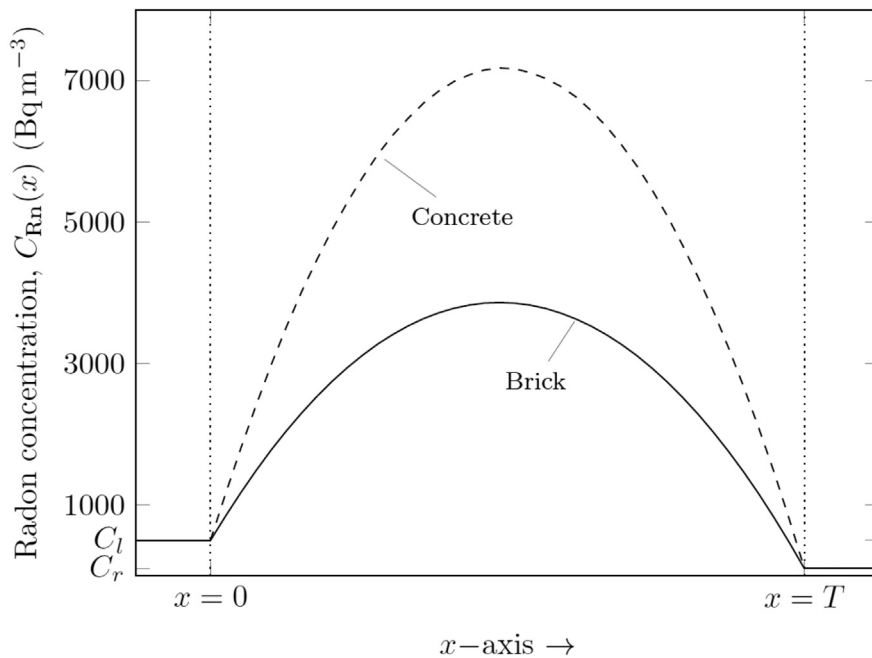

Fig. 3. Radon concentration function along x-axis in steady-state for slabs made of bricks and concrete. The following values have been assumed for concrete (i) and brick (ii), respectively: i) $f = 0.24$ (Nuccetelli et al., 2017), $R = 0.69$ m (Keller et al., 2001), $\varepsilon = 0.2$ (Li et al., 2021), $C_{Ra-226} = 59$ Bq kg^{-1} (Trevisi et al., 2018), $\rho = 2.4$ g cm^{-3} (Dorf, 2004); ii) $f = 0.12$ (Nuccetelli et al., 2017), $R = 0.41$ m (Keller et al., 2001), $\varepsilon = 0.35$ (Hall and Hamilton, 2013), $C_{Ra-226} = 51$ Bq kg^{-1} (Trevisi et al., 2018), $\rho = 1.9$ g cm^{-3} (Dorf, 2004). All the symbols are defined in Appendix A.

The corresponding exhalation rate on the left side of the slab can be computed considering the opposite versus of the x-axis relative to the exhalation process: this reflects on to the minus before dx.

$$E(0) = -D\frac{dC_{\text{Rn}}(x)}{-dx}\Big|_{x=0}$$
$$= \frac{Dr}{\sinh(rT)}\left\{C_r - C_l\cosh(rT) + \frac{G_v}{\lambda_{\text{Rn}}}[\cosh(rT) - 1]\right\} \quad (12)$$

Equivalent equations have been provided by Font (1997) although with different mathematical formulations.

This scenario extends the applicability of the general equations obtained in Section 3.1.1 by considering not negligible the inner production of radon as it happens in most of the building materials used both for perimetral and partition walls (Trevisi et al., 2018).

3.2.2. Fixed concentration on a side of an infinite slab

Considering the reference system of Fig. 4, the migration of radon through an infinite porous medium with inner radon generation can be modelled by considering the following boundary conditions:

$$\begin{cases} C_{\text{Rn}}(x = 0) = C_0 \\ C_{\text{Rn}}(x \to \infty) = C_{max} \end{cases} \quad (13)$$

where C_{max} equals $\frac{G_v}{\lambda_{\text{Rn}}}$ by considering Eq. (9). The absolute air pressures at $x = 0$ and $x \to \infty$ are assumed to be the same, i.e., $p_0 = p_s$. The general solution of radon concentration results from Eq. (9).

$$C_{\text{Rn}}(x) = C_0 e^{-rx} + \frac{G_v}{\lambda_{\text{Rn}}}(1 - e^{-rx}) \quad (14)$$

Fig. 5 shows the radon concentration function in an infinite slab for different values of the saturation degrees, i.e., the fraction of pore volume filled with water. The inner radon production rate fixed, the resulting function gets less steep with decreasing saturation degree (Abd Ali et al., 2019).

The exhalation happens only from the surface at $x = 0$. The exhalation rate, E (Bq m^{-2} s^{-1}), is computed as:

$$E(T) = -D\frac{dC_{\text{Rn}}(x)}{-dx}\Big|_{x=0} = \frac{\varepsilon\lambda_{\text{Rn}}}{r}\left(\frac{G_v}{\lambda_{\text{Rn}}} - C_0\right) \quad (15)$$

As previously introduced, this scenario has been commonly adopted for the radon exhalation rate from the soil (Nero and Nazaroff, 1984): in this scenario the radon production rate is generally significant – although rare examples exist of radon production rate neglected (e.g., (Suaro, 2014)) – and the advective transport negligible because the absolute air pressure difference between the pores space and the atmosphere is very low (Chitra et al., 2019; Speelman et al., 2004).

If the radon concentration at the surface is much less than the asymptotic level reached in the material, Eq. (15) assumes the particular formulation reported by Nero and Nazaroff (Nero and Nazaroff, 1984):

$$E(0) = \varepsilon R G_v \quad (16)$$

3.2.3. Finite slab inside a vessel with unknown radon concentration inside

This scenario was firstly introduced by Jonassen and McLaughlin (Jonassen and McLaughlin, 1980) to assess the radon exhalation rate from a sample enclosed in a vessel. The same boundary conditions were considered applicable to a wall dividing two spaces whose volume is much greater than the pore volume inside the slab (Nazaroff and Nero, 1988).

Assuming the same radon concentration on both sides of the slab entails the concentration inside the slab to be symmetrical relative to the y-z plane at $x = 0$ (Fig. 6), i.e., the $C_{\text{Rn}}(x)$ is an even function. At the steady-state, the radon exhalation equals its decay, so the radon concentration keeps
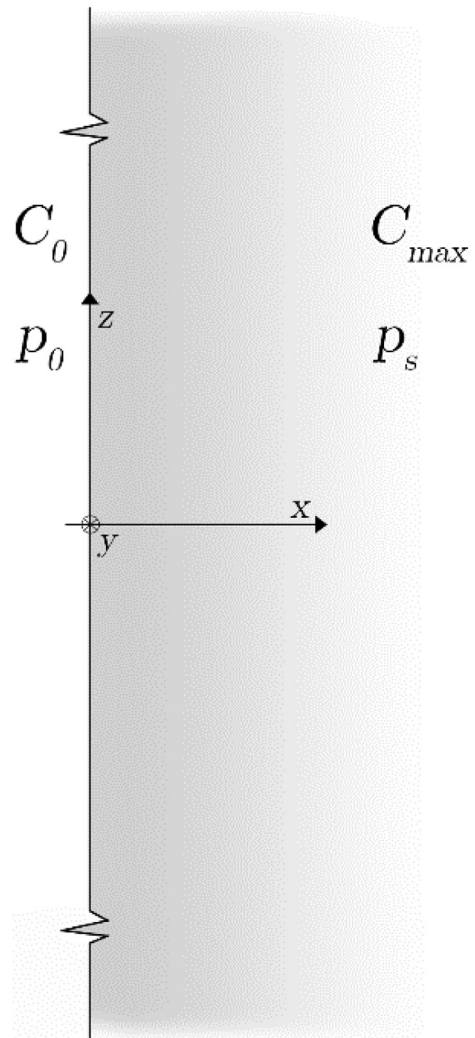

Fig. 4. Schematic representation of an infinite slab made of a porous material. The left-side surface is free to exhale into the adjacent space whose radon concentration is C_0. The free surface is at $x = 0$ and the abscissa x grows towards the porous material bulk. The radon concentration per unit pore volume at infinite depth is C_{max}. p_0 and p_s denote the absolute pressure at $x = 0$ and at x $\to \infty$, respectively.

constant over the time and uniform inside the vessel. The resulting boundary conditions are:

$$\begin{cases} C_{\text{Rn}}(x) = C_{\text{Rn}}(-x) \text{ for} -T < x < T \\ E(T)2S = C(T)V_d\lambda_{\text{Rn}} \end{cases} \quad (17)$$

where V_d is the vessel free volume, T the slab half-thickness and S the slab surface orthogonal to x-axis. The radon concentration in the vessel free volume equals the concentration per unit pore volume at $x = T$, i.e., $C(T)$.

These boundary conditions considered, the solution of Eq. (9) is:

$$C_{\text{Rn}}(x) = \frac{G_v}{\lambda_{\text{Rn}}}\left[1 - \frac{\cosh(rx)}{\cosh(\beta) + \frac{1}{\alpha\beta\sinh(\beta)}}\right] \quad (18)$$

where:

- $\alpha = \frac{V_d}{\varepsilon V_s}$ is the ratio of the vessel free volume to the pore volume of the slab and $V_S = 2ST$ is the volume of the slab;
- $\beta = rT = \frac{T}{R}$ is the ratio of the slab half-thickness to the material diffusion length (see Eq.s 42 and 43 in Appendix A).
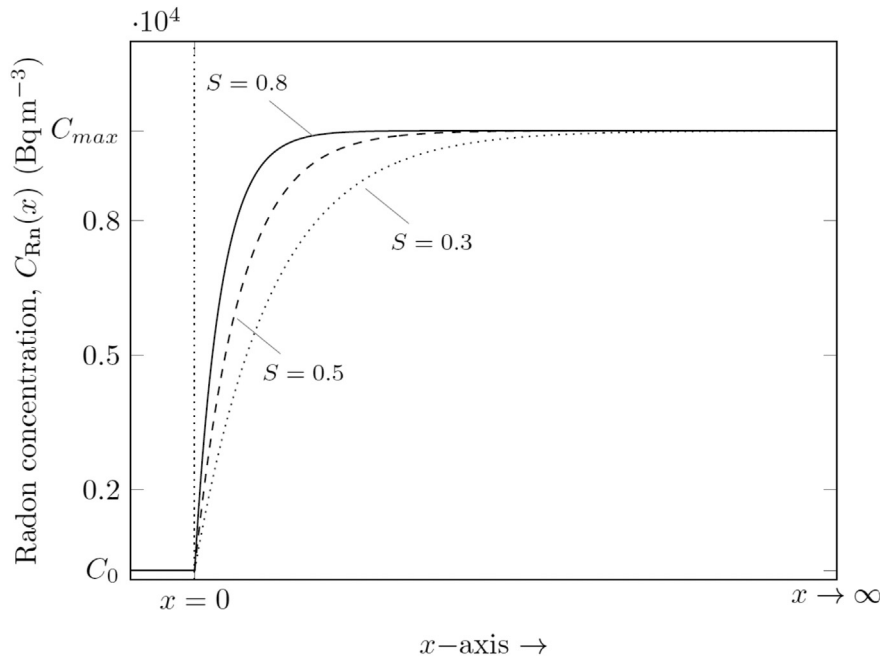
Fig. 5. Radon concentration function in steady-state for different saturation degrees, S. The diffusion length decreases as *S* increases: $R = 1.2$ m if $S = 0.3$, $R = 0.71$ m if $S = 0.5$ and $R = 0.41$ m if $S = 0.8$ (Abd Ali et al., 2019). The diffusion length is computed according to Rogers and Nielson (Rogers and Nielson, 1992). All the symbols are defined in Appendix A.
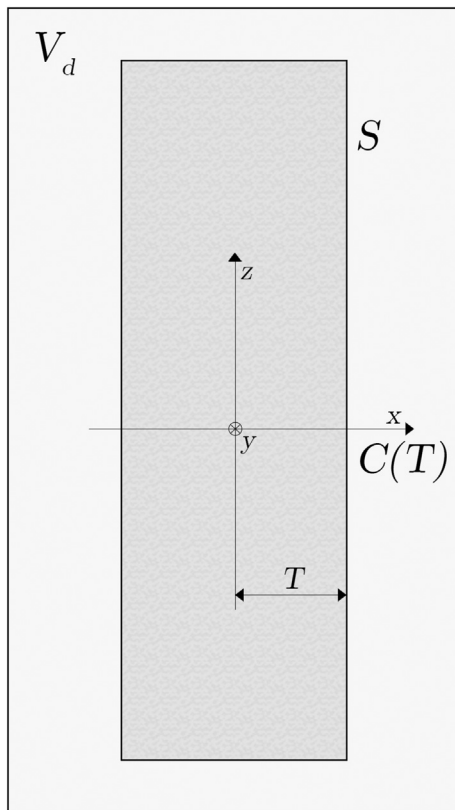

Fig. 6. Schematic representation of a slab made of a porous material and places inside a vessel. V_d is the vessel free volume computed by subtracting the slab volume V_s to the vessel volume. The thickness of the slab is assumed to be much smaller than both its height and width. The exhaling surface is $2S$.

If $V_d \gg \varepsilon V_s$, i.e., the vessel free volume is much higher than the pore volume of the slab, $\alpha \to \infty$, thus the radon concentration function becomes:

$$C_{\mathrm{Rn}}(x) = \frac{G_v}{\lambda_{\mathrm{Rn}}}\left[1 - \frac{\cosh(rx)}{\cosh(\beta)}\right] \tag{19}$$

Fig. 7 shows the differences in the resulting radon concentration trends obtained in a finite slab made of two different depending on the negligibility of slab pore volume. In this scenario, the radon exhales from both the transversal surfaces at $x = -T$ and $x = T$.

$$E(T) = -D\frac{dC_{\mathrm{Rn}}(x)}{dx}\bigg|_{x=T} = E(-T) = -D\frac{dC_{\mathrm{Rn}}(x)}{-dx}\bigg|_{x=-T} = \varepsilon RG_v\tanh(\beta) \tag{20}$$

The resulting exhalation rate is the same at the two exhaling surfaces. This formulation of the radon exhalation rate is applicable in case of rooms not completely sealed (Jonassen and McLaughlin, 1980), or rooms with large inner volume, and if the wall divides two spaces with similar radon concentration and no significant advective transport occurs. Nevertheless, it is the most widely used when assessing the radon exhalation rate from walls (e.g., (Sahoo et al., 2011; Orabi, 2018)) regardless the applicability of the underlying assumptions.

In case the wall has a pore volume comparable to the volume of spaces it divides, the exhalation rate should be assessed through the following:

$$E(T) = E(-T) = \varepsilon RG_v\frac{\tanh(\beta)}{1 + \frac{\tanh(\beta)}{\alpha\beta}} \tag{21}$$

3.3. Radon diffusive and advective transport through a slab without inner radon generation

Considering the diffusion as the only mechanism of radon transport may lead to underestimation of the actual indoor radon activity concentration: radon is effectively transported by advection throughout holes, cracks, penetrations and building materials porosities too (Font and Baixeras, 2003).
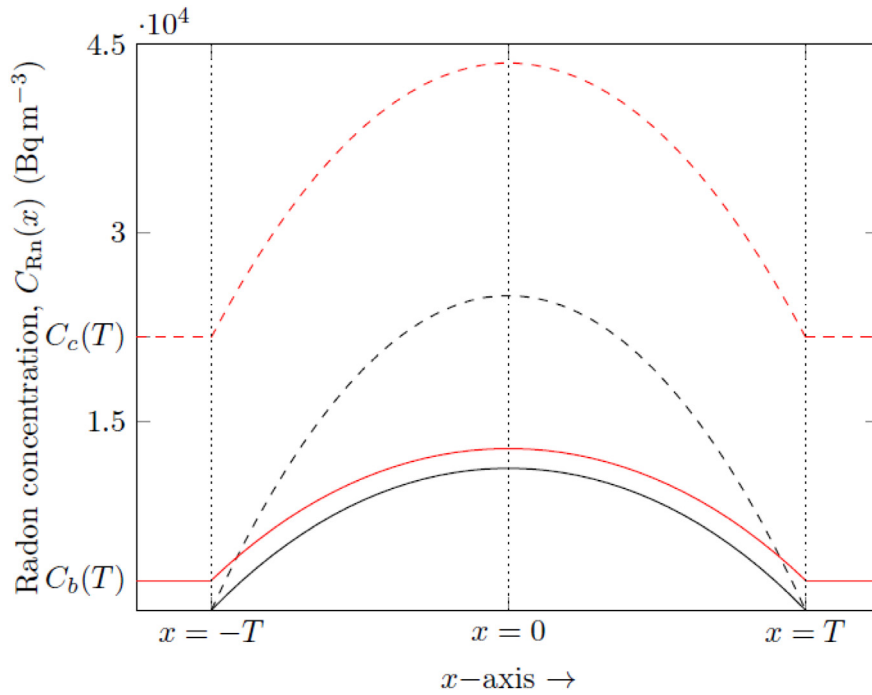
Fig. 7. Radon concentration function along x-axis in steady-state for walls made of bricks (full line) and concrete (dashed line) if the condition $V_d \gg \varepsilon V_s$ is verified (black) or not (red). The following values have been assumed for concrete (i) and brick (ii), respectively: i) $f = 0.24$ (Nuccetelli et al., 2017), $R = 0.69$ m (Keller et al., 2001), $\varepsilon = 0.2$ (Li et al., 2021), $C_{Ra-226} = 59$ Bq kg^{-1} (Trevisi et al., 2018), $\rho = 2.4$ g cm^{-3} (Dorf, 2004); ii) $f = 0.12$ (Nuccetelli et al., 2017), $R = 0.41$ m (Keller et al., 2001), $\varepsilon = 0.35$ (Hall and Hamilton, 2013), $C_{Ra-226} = 51$ Bq kg^{-1}, (Trevisi et al., 2018) $\rho = 1.9$ g cm^{-3} (Dorf, 2004). All the symbols are defined in Appendix A.

The relative contribution of this migration mechanism increases with increasing pressure gradient between the sides of building structure.

If the pressure gradient is supposed to be negligible along y- and z-axis, the radon activity concentration inside the slab can be modelled along the x-axis as it follows:

$$\frac{D_e d^2 C_{Rn}(x)}{dx^2} - \lambda_{Rn} C_{Rn}(x) \pm \frac{k}{\mu \varepsilon} \frac{dp}{dx} \frac{dC_{Rn}(x)}{dx} = 0 \qquad (22)$$

Where:

− ε is the porosity of the material the slab is made of,
− $\frac{dp}{dx}$ is the pressure gradient along the x-axis (Pa m^{-1}),
− k is the permeability of the porous material (m^2),
− μ is the carrying fluid dynamic viscosity (Pa s).

The sign of the advective term $\frac{k}{\mu \varepsilon} \frac{dp}{dx} \frac{dC_{Rn}(x)}{dx}$ is positive if the concentration and the pressure gradient are equally oriented, and negative otherwise.

The differential Eq. (22) is homogeneous and the corresponding solution is:

$$C_{Rn} = e^{\mp Mx}(Ae^{Nx} + Be^{-Nx}) \qquad (23)$$

with:

$$M = \frac{k}{\mu} \frac{\nabla p}{2D} \qquad (24)$$

$$N = \sqrt{\frac{k^2 (\nabla p)^2}{\mu^2 4D^2} + \frac{\lambda_{Rn} \varepsilon}{D}} \qquad (25)$$

3.3.1. Fixed radon concentration on both sides of a finite slab

Referring to Fig. 1, the boundary conditions are those introduced by Eq. (3) but the absolute air pressures on the sides of the slab are different, i.e., $p_l > p_r$.

The resulting general solution for radon concentration, obtained from Eq. (23), requires these boundary conditions to be considered as well as the sense of the pressure gradient.

$$C_{Rn}(x) = \frac{e^{-Mx}}{2\sinh(NT)} \left[\frac{C_r}{e^{-MT}} \sinh(Nx) + C_l \sinh(N(T-x)) \right] \qquad (26)$$

Fig. 8 shows the radon concentration function inside the slab for two different materials under a pressure difference of 5 Pa.

The exhalation rate, E (Bq m^{-2} s^{-1}), is computed at $x = T$ as the sum of diffusive and convective contributions (Eqs. (44) and (46), respectively).

$$E(T) = E(T)^{\text{diff}} + E(T)^{\text{adv}} = -D\frac{dC_{Rn}(x)}{dx}\Big|_{x=T} - \frac{C_{Rn}(x)}{\varepsilon \mu} \frac{k}{dx}\frac{dp}{dx}\Big|_{x=T} \qquad (27)$$

$$E(T) = D \left(\frac{NC_l e^{-MT}}{\sinh(NT)} + MC_r - NC_r \coth(NT) \right) - \frac{C_{Rn}(T)k}{\varepsilon \mu} \frac{dp}{dx}\Big|_{x=T} \qquad (28)$$

This solution has been rarely adopted to model the radon exhalation from slabs: e.g., Chauhan and Kumar (Chauhan and Kumar, 2015) obtained the solution in the framework of an activity aiming to measure the radon diffusion coefficient.

3.4. Radon diffusive and advective transport through a slab with inner radon generation

The activity concentration of radium-226 and the radon emanation fraction, as previously discussed, are generally not negligible: some authors added the production term G_v to Eq. (22) to consider the diffusive and advective migration of radon generated inside the slab too (López-Coto et al., 2014; Várhegyi et al., 2012). In steady-state, if the pressure gradient is
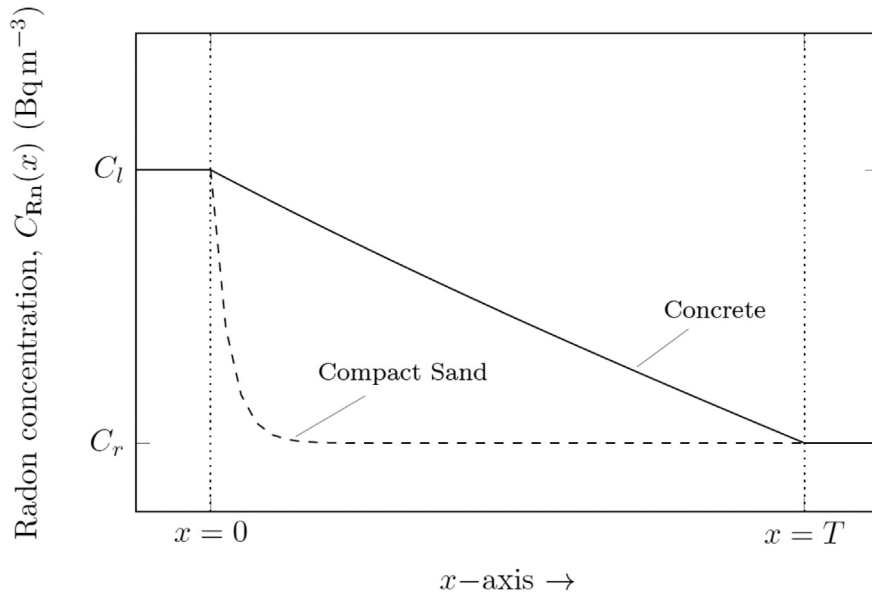
Fig. 8. Radon concentration function along $x-$ axis in steady-state under a pressure gradient of 5 Pa. The following values have been assumed for concrete (i) and compact sand (ii), respectively: i) $R = 0.69$ m (Keller et al., 2001), $\varepsilon = 0.2$ (Li et al., 2021), $k = 10^{-16}$ m² (Rogers and Nielson, 1992; Renken and Rosenberg, 1995); ii) $R = 0.41$ m (Keller et al., 2001), $\varepsilon = 0.15$ (Hall and Hamilton, 2013), $k = 10^{-10}$ m² (Turtiainen, n.d.). The dynamic viscosity is assumed to be $\mu = 1.8 \cdot 10^{-5}$ Pa s (Dixon, 2007). All the symbols are defined in Appendix A.

supposed to be negligible along *y*- and *z*-axis, the radon concentration along the *x*-axis inside a porous material is:

$$D_e \frac{d^2 C_{Rn}(x)}{dx^2} - \lambda_{Rn} C_{Rn}(x) \pm \frac{k}{\mu \varepsilon} \frac{dp}{dx} \frac{dC_{Rn}(x)}{dx} + G_v = 0 \qquad (29)$$

As in Eq. (22), the advective term is positive if the concentration and the pressure gradient have the same direction and sense, and negative otherwise. The general solution of the differential equation gives the most comprehensive formulation of the radon concentration function inside a slab.

$$C_{Rn}(x) = e^{\mp Mx} \left(A e^{Nx} + B e^{-Nx} \right) + \frac{G_v}{\lambda_{Rn}} \qquad (30)$$

where *M* and *N* are the same quantities previously introduced by Eqs. (24) and (25).

3.4.1. Fixed radon concentration on both sides of a finite slab

Referring to Fig. 1, the boundary conditions are the same already seen in Section 3.3.1. The radon concentration function results from Eq. (30) considering the boundary conditions and the sense of the pressure gradient:

$$C_{Rn}(x) = \frac{e^{-Mx}}{\sinh(NT)} \left\{ \frac{C_r - \frac{Gv}{\lambda_{Rn}}}{e^{-MT}} \sinh(Nx) - \left(C_l - \frac{G_v}{\lambda_{Rn}} \right) \sinh[N(x-T)] \right\} + \frac{G_v}{\lambda_{Rn}} \quad (31)$$

Fig. 9 shows the radon concentration function inside the slab for two different materials under a pressure difference of 5 Pa.

The exhalation rate, E (Bq m^{-2} s^{-1}), is computed at $x = 0$ and $x = T$ as the sum of diffusive and convective contributions (Eqs. (44) and (46), respectively).

$$E(0) = D \left\{ -N \left(C_l - \frac{G_v}{\lambda_{Rn}} \right) \coth(NT) - M \left(C_l - \frac{G_v}{\lambda_{Rn}} \right) \right. \qquad (32)$$
$$\left. + \frac{N \left(C_r - \frac{G_v}{\lambda_{Rn}} \right) e^{MT}}{\sinh(NT)} \right\} + \frac{C_{Rn}(0)k}{\varepsilon\mu} \frac{dp}{dx}\Big|_{x=0}$$

$$E(T) = -D \left\{ N \left(C_r - \frac{G_v}{\lambda_{Rn}} \right) \coth(NT) - M \left(C_r - \frac{G_v}{\lambda_{Rn}} \right) \right. \qquad (33)$$
$$\left. - \frac{N \left(C_l - \frac{G_v}{\lambda_{Rn}} \right) e^{-MT}}{\sinh(NT)} \right\} - \frac{C_{Rn}(T)k}{\varepsilon\mu} \frac{dp}{dx}\Big|_{x=T}$$

Referring to Fig. 9, the source term, i.e., the radon production rate in pores, is about the same for compact sand and concrete. The different radon activity concentration shape is mainly due to the extremely different (i.e., six orders of magnitude higher for compact sand) air permeability. A lower permeability reflects on a much weaker capability of the pressure-driven air flow to transport radon from inside the slab to outside. When the radon is less effectively transported outside, it keeps inside the slab and its activity concentration assumes the parabolic shape shown in Fig. 9. Oppositely if the permeability is high, the radon atoms are effectively transported outside the slab and the resulting inner activity concentration goes rapidly to the lower value on the slab sides. Thus, strong changes on the gas permeability can result in the advective and the diffusive flows to be directed the same or opposite way due to change in radon concentration shape near the side with the higher radon outside concentration.

This scenario is generally applicable to all the building structures, both partition and perimetral ones, to assess the radon concentration distribution inside the building material, the corresponding exhalation rate and the resulting contribution to the indoor radon concentration. The solutions previously presented in Section 3.1.1, Section 3.2.1 and Section 3.3.1 can be obtained from Eqs. (31), (32) and (33) by simplifying the advection and/or the inner production terms. Eq. 32 extends the applicability of the scenarios in Section 3.1.1 and Section 3.2.1 by considering also the advective transport.

3.4.2. Fixed concentration on a side of an infinite slab

The reference system of Fig. 4 considered, the diffusive and advective migration of radon throughout an infinite porous medium with inner radon generation can be modelled by considering the boundary conditions in Eq. (12). The absolute air pressure inside the slab is supposed to be
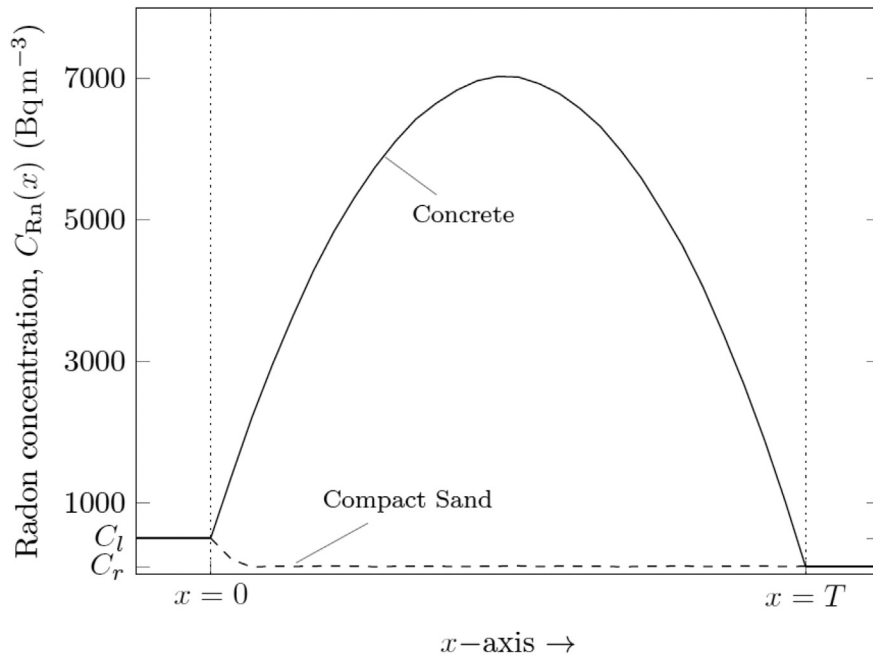
Fig. 9. Radon concentration function along x-axis in steady-state under a pressure gradient of 5 Pa. The following values have been assumed for concrete (i) and compact sand (ii), respectively: i) $f = 0.24$ (Nuccetelli et al., 2017), $R = 0.69$ m (Keller et al., 2001), $\varepsilon = 0.2$ (Li et al., 2021), $C_{Ra-226} = 59$ Bq kg^{-1} (Trevisi et al., 2018), $\rho = 2.4$ g cm^{-3} (Dorf, 2004), $k = 10^{-16}$ m^2 (Rogers and Nielson, 1992; Renken and Rosenberg, 1995); ii) $f = 0.24$ (Seco et al., 2020), $R = 0.41$ m (Keller et al., 2001), $\varepsilon = 0.15$ (Hall and Hamilton, 2013), $C_{Ra-226} = 71$ Bq kg^{-1} (Seco et al., 2020), $\rho = 2.45$ g cm^{-3} (Manger, 1963), $k = 10^{-10}$ m^2 (Turtiainen, n.d.). The dynamic viscosity is assumed to be $\mu = 1.8 \cdot 10^{-5}$ Pa s (Dixon, 2007). All the symbols are defined in Appendix A.

higher than the outside value, i.e., $p_s > p_0$. The resulting radon concentration function obtained from Eq. (30) is:

$$C_{Rn}(x) = C_0 e^{-(N+M)x} + \frac{G_v}{\lambda_{Rn}}\left(1 - e^{-(N+M)x}\right) \qquad (34)$$

The radon concentration function inside the slab is plotted in Fig. 10 to highlight the influence of the saturation degree with fixed radon production rate. The increase of the pressure gradient reflects on a steeper slope of the radon concentration function.
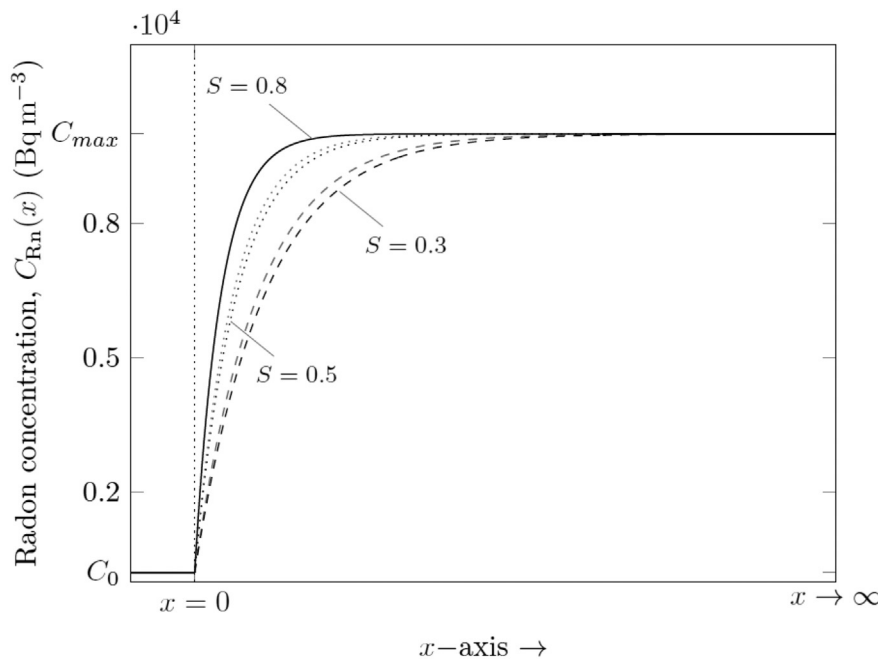
Fig. 10. Radon concentration function in steady-state in a silty soil with different saturation degrees S. The values of the diffusion length R are the same as Fig. 6. The permeability of dry soil has been obtained from the Kozeny theory (Nazaroff, 1992) and the values at different saturation degrees by considering the fitting function e^{-12S^4} (Rogers and Nielson, 1991). The black and red curves have been obtained considering a pressure gradient of 5 and 10 Pa, respectively. The porosity has been set to 0.5 (Nazaroff, 1992).

The exhalation happens only from the surface at $x = 0$ at the rate (Bq m^{-2} s^{-1}):

$$E(0) = D(N + M)\left(\frac{G_v}{\lambda_{\text{Rn}}} - C_0\right) - k\frac{C_{\text{Rn}}(0)}{\varepsilon\mu}\frac{dP}{-dx}\Bigg|_{x=0} \qquad (35)$$

If the radon concentration at the surface is much less than the asymptotic level reached in the material, Eq. (35) turns into:

$$E(0) = D\,(N + M)\frac{G_v}{\lambda_{\text{Rn}}} + k\frac{C_{\text{Rn}}(0)}{\varepsilon\mu}\frac{dp}{-dx}\Bigg|_{x=0} \qquad (36)$$

This scenario extends the applicability of the solutions obtained in the case of only diffusive radon transport (Section 3.2.2) by including the contribution of the advective transport. Eqs. (34) and (35) are generally applicable to building structures attached to the underlying soil and comprehensively consider the effect of the pressure gradient in enhancing or reducing the relative contribution to the indoor radon concentration.

4. Discussion

Four models have been developed to describe the radon exhalation phenomena from building structures. The models differ for the migration mechanisms considered – i.e., only diffusive, or diffusive and advective – and the presence of radon generation inside the building material. Each of these models was analytically solved for some case-specific scenarios likely to occur in dwellings and workplaces and an equation to estimate radon exhalation from building structures was derived.

The provided solutions have been obtained under some simplifying conditions that need to be discussed as well as the resulting limitation of the proposed approach.

The general transport equation for radon migration reported in Annex A (Eq. (37)) was employed. This formulation implies some simplifications, especially the negligibility of moisture content and the isotropy and homogeneity of the porous media. The applicability of the resulting formulations is restricted to the same simplifications.

Furthermore, the 1-D modelling has been adopted to represent the exhalation phenomenon. This is typically justified considering that the radon concentration and pressure gradient mainly occur along the axis perpendicular to the wall, and that the thickness of the slab is much smaller than its height and width. However, specific circumstances exist in which the applicability of the provided equations need to be specifically addressed, e.g., in case of walls with non-uniform thickness or radium-226 concentration.

Finally, the applicability of the equations provided to assess the radon exhalation rate is limited to raw building structures, i.e., with simple or no surface treatments. Where there is a covering on the wall (e.g., mortar, plaster, or paint), the provided equations may lead to overestimated assessments of the actual radon exhalation rate (Yu, 1993) or even to underestimation in case of covering layers containing high radium-226 concentration, e.g., tiles and granite (Chen et al., 2010).

5. Conclusions

The present paper contains a general and comprehensive discussion of the theoretical background underlying the radon transport and exhalation phenomena. A system analysis has been carried out about the models to describe the transport of radon inside porous materials and its exhalation from structures: the work has resulted in four formulations depending on the migration mechanisms considered – i.e., only diffusive, or diffusive and advective – and the contribution of the inner radon production. For each of these models, the general solution has been analytically derived, and the case-specific solutions obtained by considering three sets of boundary conditions. The resulting scenarios are suitable to describe the physical phenomenon of radon exhalation from materials used in building structures of dwellings and workplaces.

The availability of case-specific solutions allows to choose the formulation best-fitting the existing scenario when assessing the radon exhalation, rather than adopting standard solution obtained under simplified conditions. The resulting accurate assessment of the radon exhalation rate from walls and other building structures, e.g., floor and ceilings, results in a reliable estimation of the contribution of building materials to the indoor radon concentration. This leads to an improvement of both preventive and remediation strategies aiming to reduce the exposure to radon indoors. Moreover, the possibility to consider the site-specific installation conditions in addition to the material properties allows to assess the health impact of building materials, including those containing NORM (Naturally Occurring Radioactive Materials) industry by-products, in actual scenarios. Nevertheless, the direct measurement of radon exhalation rate from building structure and the resulting indoor radon concentration should be always preferred due to the complexity of the actual scenario to model. The modelling approach should be considered when the indoor radon concentration measurements are not feasible (e.g., house not built yet) and to distinguish the contributions of the different radon sources (e.g., during the design of remedial strategies).

The numerical impact of the application of the case-specific solutions has been evaluated by the authors. The complexity of the results suggests discussing them on separate report where the scenarios considered will be described as well as the results obtained relative to the radon exhalation rate and the corresponding contribution to the indoor radon. The discussion will consider the improvement in the assessment's accuracy compared to the increase in the computation complexity due to the input parameters required.

CRediT authorship contribution statement

C. Di Carlo: Conceptualization, Methodology, Software, Formal analysis, Investigation, Data curation, Writing – original draft, Writing – review & editing, Visualization, Supervision. **A. Maiorana:** Conceptualization, Methodology, Software, Formal analysis, Writing – review & editing, Visualization. **M. Ampollini:** Writing – review & editing, Resources. **S. Antignani:** Software, Formal analysis. **M. Caprio:** Software, Formal analysis. **C. Carpentieri:** Writing – review & editing, Visualization. **F. Bochicchio:** Conceptualization, Writing – review & editing, Supervision, Resources, Project administration.

Data availability

No data was used for the research described in the article.

Declaration of competing interest

The authors declare that they have no known competing financial interests or personal relationships that could have appeared to influence the work reported in this paper.

Appendix A. Radon migration mechanisms and related quantities

For porous media with negligible moisture content, a general transport equation for radon migration can be expressed as follows (Nazaroff and Nero, 1988):

$$D_e\nabla^2 C_{\text{Rn}} \pm \frac{k}{\mu\varepsilon}\nabla\boldsymbol{P}\cdot\nabla\boldsymbol{C_{\text{Rn}}} + G_v - \lambda_{\text{Rn}}\,C_{\text{Rn}} = \frac{dC_{\text{Rn}}}{dt} \qquad (37)$$

where:

- D_e is the effective diffusivity of porous medium along the x-axis (m^2 s^{-1}),
- ε is the medium porosity,
- C_{Rn} is the activity concentration of radon per unit volume of interstitial space (Bq m^{-3}) and $\nabla\boldsymbol{C_{\text{Rn}}}$ the corresponding gradient vector,

- λ_{Rn} is the radon decay constant (s^{-1}),
- ∇P is the absolute pressure gradient vector (Pa m^{-1}),
- k is the permeability of the porous material (m^2),
- μ is the carrying fluid (i.e., mainly the air) dynamic viscosity (Pa s),
- G_v is the radon emanation rate, or the radon production rate, per unit pore volume (Bq s^{-1} m^{-3}).

The first term on the left accounts for the variation of radon concentration by diffusive flow whereas the second one refers to effect of the convective transport.

Eq. (37) relies on some simplifying assumptions: (*i*) water content is assumed negligible, i.e., all pores are air-filled so the migration of radon occurs in air, (*ii*) no adsorption of radon atoms is assumed to occur on the surfaces of the solid grains, and (*iii*) radon is assumed to migrate only down its concentration gradient and/or the air pressure gradient. Furthermore, porous media are supposed to be isotropic and homogeneous relative to diffusion coefficient, permeability, porosity, emanation coefficient, radium content, and bulk density.

If the radon fraction in water-filled pores is assumed negligible, the radon production rate per unit pore volume can be expressed by (Nazaroff and Nero, 1988):

$$G_v = \frac{1}{\varepsilon} C_{\mathrm{Ra}} \rho f \lambda_{\mathrm{Rn}} \tag{38}$$

where:

- C_{Ra} is the activity concentration of radium-226 per unit mass of the material (Bq kg^{-1}),
- ρ is the density of the material (kg m^{-3}),
- f is the emanation coefficient,
- λ_{Rn} is radon decay constant (s^{-1}).

The factor $\frac{1}{\varepsilon}$ is introduced to move from radon production rate per unit bulk volume to the corresponding rate per unit pore volume. Other authors considers $\frac{1-\varepsilon}{\varepsilon}$ in place of $\frac{1}{\varepsilon}$ (Font, 1997).

A.1. Diffusive transport

The diffusive transport refers to the migration of a molecular species down its concentration gradient (Nazaroff and Nero, 1988). The Fick's Law governs such a molecular motion through the so-called diffusion coefficient (sometimes referred to as molecular diffusivity). The diffusion coefficient in open air, D_0, needs to be adjusted when addressing migration in porous media to consider two different phenomena:

i) the presence of solid particles (in porous media generally referred to as "grains") causes the diffusion paths of species to deviate from straight lines. The diffusion coefficient must be adjusted to account for the deviations by the tortuosity factor defined as the actual distance travelled by the species (l) per unit length of the medium crossed (x), $\tau = \frac{\Delta l}{\Delta x}$ (Shen and Chen, 2007). Dullien (Dullien, 1979) defines the tortuosity factor as $\tau = \frac{\Delta l^2}{\Delta x^2}$.
ii) The cross-sectional area the diffusion occurs through is reduced by the presence of the grains. This reduction is accounted by a fraction equal to the ratio of the open pore area, A^*, to the total cross section, A, i.e., the areal porosity (Nimmo, 2004) (Open pore area at a given cross-section of a porous material: rearrangement from Culot, Olson and Schiager (Culot et al., 1976) (Fig. 11).

The bulk coefficient, in the following referred to as D, is introduced to account for the lengthening of the path travelled (i). It relates the gradient of interstitial concentration of diffusing radon (becquerel per cubic meters of pore volume) to the flux density over the cross-sectional area (becquerel
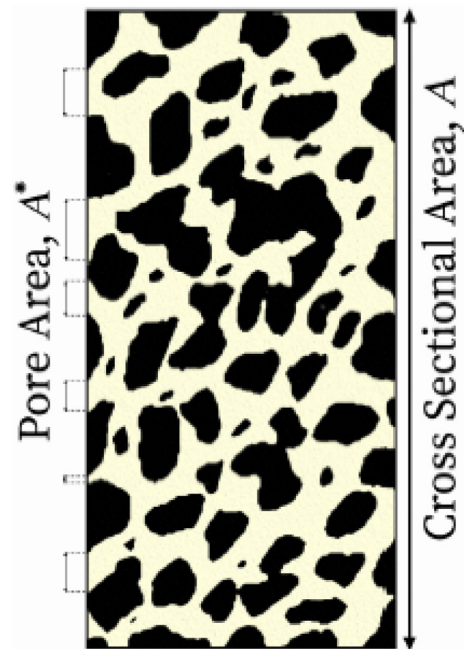

Fig. 11. Open pore area at a given cross-section of a porous material: rearrangement from Culot, Olson and Schiager (Culot et al., 1976).

per square meters of the cross-section). According to Shen and Chen (Shen and Chen, 2007):

$$D = D_0 \, \tau^2 \tag{39}$$

In case of high porous media, τ was found to be well fitted by the porosity ε, so $\tau^2 \approx \varepsilon^2$ (Ullman and Aller, 1982). It results (Buckingham and B.o.S. U.S. Dept. of Agriculture, 1904):

$$D = D_0 \, \varepsilon^2 \tag{40}$$

Other correlations have been proposed for $\tau(\varepsilon)$ (Shen and Chen, 2007; Matyka et al., 2008).

The effective coefficient, in the following referred to as D_e, is introduced to account for the reductions in cross-sectional area (ii) and it relates the gradient of interstitial concentration of diffusing radon (becquerel per cubic meters of pore volume) to the flux density over the cross-sectional pore area (becquerel per square meters of the cross-section). D_e is related to D by the following relationship:

$$D_e = D \frac{A}{A*} \approx D \frac{V}{V_v} = \frac{D}{\varepsilon} \tag{41}$$

where:

- V is the overall volume of the porous material (m^3),
- V_v is the void volume of the porous material, both water- and gas-filled (m^3),
- ε is the material porosity.

The assumption underlying Eq. (41) is the equality between the areal porosity (i.e., the fraction of open pore area in a unit cross-section) and the volume porosity, i.e., $\frac{A}{A^*} \approx \frac{V}{V^*} = \varepsilon$ (Culot et al., 1976): the assumption is legit in case of porous media with random structure (Dullien, 1979).

Rather than the diffusion coefficient, some authors prefer using the diffusion length, R, or its inverse, r (e.g., (Jonassen and McLaughlin, 1980)):

$$R = \sqrt{\frac{D_e}{\lambda_{\mathrm{Rn}}}} \tag{42}$$

$$r = \frac{1}{R} = \sqrt{\frac{\lambda_{Rn}}{D_e}} \qquad (43)$$

The diffusion of radon in isotropic and homogeneous porous media is modelled by the first Fick's law:

$$\boldsymbol{J}_{\mathbf{Rn}}^{d} = -D_e \boldsymbol{\nabla} \boldsymbol{C}_{\mathbf{Rn}} \qquad (44)$$

where:

- $\boldsymbol{J}_{\mathbf{Rn}}^{d}$ is the diffusive flux density vector of radon activity per unit pore area of the material (Bq m^{-2} s^{-1}),
- D_e is the effective diffusion coefficient (Shen and Chen, 2007) (m^2 s^{-1}),
- C_{Rn} is the activity concentration of radon per unit volume of interstitial space (Bq m^{-3}) and $\boldsymbol{\nabla} \boldsymbol{C}_{\mathbf{Rn}}$ the corresponding gradient vector.

Radon migration can be modelled by Eq. (44) under two main assumptions:

i) all the kinetic interactions of radon atoms happen as in the open air, i.e., with other gas molecules and not with the solid boundaries of grains (Nazaroff and Nero, 1988). The reasonability of this assumption depends on the recoil range of radon atoms (Tanner, 1980; Wilkening, 1990) relative to the dimension of open pores. When pore diameters are mostly lower than the recoil range of radon, as it happens for most building materials, the gaseous atoms collide with the wall rather than colliding with other atoms. The resulting diffusion coefficient of radon in open air (D_0) is substituted by the Knudsen diffusivity – strongly dependent on the position within the pores (Youngquist, 2002) – to consider the pores diameter (Knudsen, 1909).

ii) All the radon atoms are entirely either in the air filling the voids or in the solid matrix (Nazaroff and Nero, 1988). This assumption requires the pores size distribution to be unimodal, the fraction of radon contained in water-filled pores to be negligible and no appreciable adsorption of radon atoms on solid grains to happen.

A.2. Convective transport

The convective (in literature "advective" is commonly used to denote the same mechanism) transport describes the migration of molecular species via a bulk motion governed by fluid's head difference. The convective transport is mostly driven by a pressure gradient because the effects of gravity are generally negligible for gasses in porous media. The governing equation of advection in isotropic and homogeneous porous media is the Darcy's law (Whitaker, 1986; Darcy, 1856):

$$\boldsymbol{\nu} = -\frac{k}{\mu} \boldsymbol{\nabla} \boldsymbol{P} \qquad (45)$$

where:

- $\boldsymbol{\nu}$ is the volumetric fluid flow rate vector (cm^3 s^{-1}) per unit geometrical area (cm^2) defined over a region large relative to individual pores but small to the overall dimensions of the material (m s^{-1}),
- $\boldsymbol{\nabla} \boldsymbol{P}$ is the pressure gradient vector (Pa m^{-1}),
- k is the permeability of the porous material (m^2),
- μ is the carrying fluid dynamic viscosity (Pa s).

The Eq. (45) is valid if the effects of gravity are negligible (i) and the flow through the porous material happens as a viscous flow through a pipe (ii).

Given the flow velocity, the advective transport of radon in porous media is modelled as follow:

$$\boldsymbol{J}_{\mathbf{Rn}}^{a} = \frac{C_{Rn} \boldsymbol{\nu}}{\varepsilon} = -C_{Rn} \frac{1}{\mu} \frac{k}{\varepsilon} \boldsymbol{\nabla} \boldsymbol{P} \qquad (46)$$

where:

- $\boldsymbol{J}_{\mathbf{Rn}}^{a}$ is the advective flux density vector of radon activity per unit pore area of the material (Bq m^{-2} s^{-1}),
- C_{Rn} is the activity concentration of radon per unit volume of interstitial space (Bq m^{-3}),
- ε is the porous material porosity.

The Eq. (46) implies the radon carrier, i.e., the air, to be incompressible for the range of pressures of interest (Nazaroff and Nero, 1988).

The Darcy's law has been extensively used in applications at Reynolds (*Re*) number (Wang et al., 2019) values of up to 1 (Chaudhary et al., 2011) and a general consensus exists about Darcy's law applicability for an upper limit of *Re* value between 1 and 10 for average grain size and velocity (Bear, 1975). For higher *Re* numbers, due to emerging importance of inertial forces, deviations of fluid flow from Darcy's law have been observed even if the flow keeps laminar (Muskat, 1938; Forchheimer, 1901; Dupuit, 1863). Critical values of 0.01–0.1 resulted for disordered porous media (Andrade Jr et al., 1999). For flows in porous media with Reynolds numbers greater than about 1 to 10, the inertial Forchheimer term (Forchheimer, 1901) should be added to the Darcy's equation.

The applicability of the Darcy's law requires the pores to be large relative to the mean free path of the gas to make the particle-wall interactions negligible (Carrigy et al., 2012).

References

Abd Ali, F.S., Mahdi, K.H., Jawad, E.A., 2019. Humidity effect on diffusion and length coefficient of radon in soil and building materials. In: U.o.B College of Education for Pure Science, Baghdad, Iraq (Ed.), Technologies and Materials for Renewable Energy, Environment and Sustainability, TMREES18, Athens, Greece, pp. 384–392.

Andrade Jr., J., Costa, U., Almeida, M., Makse, H., Stanley, H.J.P.R.L., 1999. Inertial effects on fluid flow through disordered porous media. 82, 5249.

Barros-Dios, J.M., Ruano-Ravina, A., Gastelu-Iturri, J., Figueiras, A., 2007. Factors underlying residential radon concentration: results from Galicia, Spain. Environ. Res. 103, 185–190.

Bear, J., 1975. Dynamics of fluids in porous media. Soil Sci. 120, 162–163.

Bochicchio, F., Campos Venuti, G., Nuccetelli, C., Piermattei, S., Risica, S., Tommasino, L., Torri, G., 1999. Results of the National Survey on radon indoors in all the 21 Italian Regions. Radon in the Living Environment (1999, April), Athens, pp. 19–23.

Buckingham, E., 1904. In: B.o.S. U.S. Dept. of Agriculture (Ed.), Contributions to our knowledge of the aeration of soils Washington, D.C.

Carrigy, N.B., Pant, L.M., Mitra, S., Secanell, M., 2012. Knudsen diffusivity and permeability of PEMFC microporous coated gas diffusion layers for different polytetrafluoroethylene loadings. J. Electrochem. Soc. 160, F81–F89.

Chaudhary, K., Cardenas, M.B., Deng, W., Bennett, P.C., 2011. The role of eddies inside pores in the transition from Darcy to Forchheimer flows. Geophys. Res. Lett. 38, n/a–n/a.

Chauhan, R.P., Kumar, A., 2015. A comparative study of indoor radon contributed by diffusive and advective transport through intact concrete. Phys. Procedia 80, 109–112.

Chen, J., Rahman, N.M., Abu Atiya, I., 2010. Radon exhalation from building materials for decorative use. J. Environ. Radioact. 101, 317–322.

Chitra, N., Sundar, S.B., Jose, M.T., Sivasubramanian, K., Venkatraman, B., 2019. A simple model to simulate the diffusion pattern of radon in different soil media. J. Radioanal. Nucl. Chem. 322, 1151–1158.

Collignan, B., Powaga, E., 2019. Impact of ventilation systems and energy savings in a building on the mechanisms governing the indoor radon activity concentration. J. Environ. Radioact. 196, 268–273.

Culot, M.V., Olson, H.G., Schiager, K.J., 1976. Effective diffusion coefficient of radon in concrete, theory and method for field measurements. Health Phys. 30, 263–270.

Darcy, H., 1856. The public fountains of the city of Dijon. Experience and application principles to follow and formulas to be used in the. I.G.O.B.A. HIGHWAYS Paris.

Denman, A.R., Groves-Kirkby, N.P., Groves-Kirkby, C.J., Crockett, R.G., Phillips, P.S., Woolridge, A.C., 2007. Health implications of radon distribution in living rooms and bedrooms in U.K. dwellings–a case study in Northamptonshire. Environ. Int. 33, 999–1011.

Dixon, J.C., 2007. Properties of air. In: Inc, J.W.S. (Ed.), The Shock Absorber Handbook, pp. 375–378.

Dorf, R.C., 2004. The Engineering Handbook.

Dullien, F.A.L., 1979. Porous Media: Fluid Transport and Fluid Structures. Academic Press Limited.

Dupuit, J., 1863. Études théoriques et pratiques sur le mouvement des eaux. Librairie des corps impériaux des ponts et chaussées et des mines, Paris.

European Commission, 2014. Council Directive 2013/59/Euratom: basic safety standards for protection against the dangers arising from exposure to ionising radiation. In: E. Commission (Ed.), Official Journal of the European Union, pp. 1–73.

Font, L., 1997. Radon generation, entry and accumultion. Grup de Fisica de les Radiacions Universitat Autònoma de Barcelona, Barcelona (Spain), p. 189.

Font, L., Baixeras, C., 2003. The RAGENA dynamic model of radon generation, entry and accumulation indoors. Sci. Total Environ. 307, 55–69.

Forchheimer, P., 1901. Wasserbewegung durch Boden. Zeitschrift des Vereins deutscher Ingenieure 45.

Frutos, B., Martín-Consuegra, F., Alonso, C., Perez, G., Peón, J., Ruano-Ravina, A., Barros, J.M., Santorun, A.M., 2021. Inner wall filler as a singular and significant source of indoor radon pollution in heritage buildings: an exhalation method-based approach. Build. Environ. 201.

Hall, C., Hamilton, A., 2013. Porosity–density relations in stone and brick materials. Mater. Struct. 48, 1265–1271.

Hsu, C.-N., Tsai, S.-C., Liang, S.-M., 1994. Evaluation of diffusion parameters of radon in porous material by flow-through diffusion experiment. Appl. Radiat. Isot. 45, 845–850.

I.O.f. Standardization, Technical report, 2012. Measurement of radioactivity in the environment — air: radon-222 — part 7: accumulation method for estimating surface exhalation rate. ISO 11665-7 2012.

IARC, 2012. Radiation: a review of human carcinogens. International Agency for Research on Cancer. IARC monographs on the evaluation of carcinogenic risks to humans. World Health Organization (WHO).

Ishimori, Y., Lange, K., Martin, P., Mayya, Y.S., Phaneuf, M., 2013. Technical Reports Series no. 474 – "Measurement and Calculation of Radon Releases from NORM Residues". International Atomic Energy Agency (IAEA), Vienna.

Iskandar, D., Yamazawa, H., Iida, T., 2004. Quantification of the dependency of radon emanation power on soil temperature. Appl. Radiat. Isot. 60, 971–973.

Jonassen, N., McLaughlin, J., 1980. Exhalation of Radon-222 from Building Materials and Walls.

Keller, G., Hoffmann, B., Feigenspan, T., 2001. Radon permeability and radon exhalation of building materials. Sci. Total Environ. 272, 85–89.

Knudsen, M., 1909. Die Gesetze der Molekularströmung und der inneren Reibungsströmung der Gase durch Röhren. Ann. Phys. 333, 75–130.

Leivo, V., Kiviste, M., Aaltonen, A., Turunen, M., Haverinen-Shaughnessy, U., 2015. Air pressure difference between indoor and outdoor or staircase in multi-family buildings with exhaust ventilation system in Finland. Energy Procedia 78, 1218–1223.

Li, L.G., Feng, J.-J., Zhu, J., Chu, S.-H., Kwan, A.K.H., 2021. Pervious concrete: effects of porosity on permeability and strength. Mag. Concr. Res. 73, 69–79.

López-Coto, I., Mas, J., Vargas, A., Bolívar, J., 2014. Studying radon exhalation rates variability from phosphogypsum piles in the SW of Spain. J. Hazard. 280, 464–471.

Lucchetti, C., Castelluccio, M., Altamore, M., Briganti, A., Galli, G., Soligo, M., Tuccimei, P., Voltaggio, M., 2020. Using a scale model room to assess the contribution of building material of volcanic origin to indoor radon. Nukleonika 65, 71–76.

Lucchetti, C., Galli, G., Tuccimei, P., 2022. Indoor/outdoor air exchange affects indoor radon – the use of a scale model room to develop a mitigation strategy. Adv. Geosci. 57, 81–88.

Manger, G.E., 1963. Porosity and bulk density of sedimentary rocks. U.S.A.E.C. Technical Report. Geological Survey Bulletin 1144-E.

Matyka, M., Khalili, A., Koza, Z., 2008. Tortuosity-porosity relation in porous media flow. Phys. Rev. E Stat. Nonlinear Soft Matter Phys. 78, 026306.

McGrath, J.A., Aghamolaei, R., O'Donnell, J., Byrne, M.A., 2021. Factors influencing radon concentration during energy retrofitting in domestic buildings: a computational evaluation. Build. Environ. 194.

Minkin, L., 2002. Is diffusion, thermodiffusion, or advection a primary mechanism of indoor radon entry? Radiat. Prot. Dosim. 102, 153–162.

Muskat, M., 1938. The flow of homogeneous fluids through porous media. Soil Sci. 46.

Nazaroff, W.W., 1992. Radon transport from soil to air. Rev. Geophys. 30.

Nazaroff, W.W., Nero, A.V., 1988. Radon and Its Decay Products in Indoor Air. Wiley-interscience publication.

Nero, A.V., Nazaroff, W.W., 1984. Characterising the source of radon indoors. Radiat. Prot. Dosim. 7, 23–39.

Nimmo, J., 2004. Porosity and pore-size distribution. Encyclopedia of Soils in the Environment, London, pp. 295–303.

Nuccetelli, C., Risica, S., Onisei, S., Leonardi, F., Trevisi, R., 2017. Natural radioactivity in building materials in the European Union: a database of activity concentrations, radon emanations and radon exhalation rates. Rapporti ISTISAN, Istituto Superiore di Sanità, Roma.

Orabi, M., 2018. Estimation of the radon surface exhalation rate from a wall as related to that from its building material sample. Can. J. Phys. 96, 353–357.

Renken, K.J., Rosenberg, T., 1995. Laboratory measurements of the transport of radon gas through concrete samples. Health Phys. 68, 800–808.

Rogers, V.C., Nielson, K.K., 1991. Correlations for predicting air permeabilities and 222Rn diffusion coefficients of soils. Health Phys. 61, 225–230.

Rogers, V.C., Nielson, K.K., 1992. Data and models for radon transport through concrete. International Symposium on Radon and Radon Reduction Technology, p. VI-3.

Rogers, V.C., Nielson, K.K., Holt, R.B., 1995. Radon diffusion coefficients for aged residential concretes. Health Phys. 68, 832–834.

Sabbarese, C., Ambrosino, F., D'Onofrio, A., 2021. Development of radon transport model in different types of dwellings to assess indoor activity concentration. J. Environ. Radioact. 227, 106501.

Sahoo, B.K., Sapra, B.K., Gaware, J.J., Kanse, S.D., Mayya, Y.S., 2011. A model to predict radon exhalation from walls to indoor air based on the exhalation from building material samples. Sci. Total Environ. 409, 2635–2641.

Seco, S.L.R., Domingos, F.P., Pereira, A., Duarte, L.V., 2020. Estimation of the radon production potential in sedimentary rocks: a case study in the Lower and Middle Jurassic of the Lusitanian Basin (Portugal). J. Environ. Radioact. 220-221, 106272.

Shen, L., Chen, Z., 2007. Critical review of the impact of tortuosity on diffusion. Chem. Eng. Sci. 62, 3748–3755.

Speelman, W.J., Lindsay, R., Newman, R.T., Joseph, A.D., et al., 2004. Modelling and measurement of radon diffusion through soil for application on mine tailings dams.pdf. VII Radiation Physics & Protection Conference, Ismailia-Egypt, pp. 279–287.

Strong, K.P., Levins, D.M., 1982. Effect of moisture content on radon emanation from uranium ore and tailings. Health Phys. 42, 27–32.

Suaro, I., 2014. Modelling of radon diffusion trough the soil. Department of Mathematics. National Institute of Technology Rourkela, Odisha, India.

Tanner, A.B., 1980. Radon migration in the ground: a supplementary review. Proc. Natural Radiation Environment III, 5.

Trevisi, R., Leonardi, F., Risica, S., Nuccetelli, C., 2018. Updated database on natural radioactivity in building materials in Europe. J. Environ. Radioact. 187, 90–105.

Tuccimei, P., Castelluccio, M., Soligo, M., Moroni, M., 2009. Radon exhalation rates of building materials: experimental, analytical protocol and classification criteria. In: Cornejo, Donald N., Haro, Jason L. (Eds.), Building Materials: Properties, Performance and Applications, pp. 259–274.

T. Turtiainen, Radon: origin, entry and affecting factors.

Ullman, W.J., Aller, R.C., 1982. Diffusion-coefficients in nearshore marine-sediments. Limnol. Oceanogr. 27, 552–556.

EPA assessment of risks from radon in homes. In: United States Environmental Protection Agency (Ed.), Office of Radiation and Indoor Air United States Environmental Protection Agency Washington DC.

UNSCEAR, 1993. Sources and effects of ionizing radiation. United Nations Scientific Committee on the Effects of Atomic Radiation (UNSCEAR) 1993 Report: Report to the General Assembly, with Scientific Annexes.

UNSCEAR, 2000. Sources and effects of ionizing radiation. United Nations Scientific Committee on the Effects of Atomic Radiation (UNSCEAR) 1993 Report: Report to the General Assembly, with Scientific Annexes.

UNSCEAR, 2006. Sources and effects of ionizing radiation. United Nations Scientific Committee on the Effects of Atomic Radiation (UNSCEAR) 2006 Report: Report to the General Assembly, with Scientific Annexes.

UNSCEAR, 2008. Sources and effects of ionizing radiation. United Nations Scientific Committee on the Effects of Atomic Radiation (UNSCEAR) 2008 Report: Report to the General Assembly, with Scientific Annexes.

Várhegyi, A., Somlai, J., Sas, Z., 2012. Radon migration model for covering U mine and ore processing tailings. First East European Radon Symposium–FERAS.

Vasilyev, A.V., Yarmoshenko, I.V., Zhukovsky, M.V., 2015. Low air exchange rate causes high indoor radon concentration in energy-efficient buildings. Radiat. Prot. Dosim. 164, 601–605.

Wang, L., Li, Y., Zhao, G., Chen, N., Xu, Y., 2019. Experimental investigation of flow characteristics in porous media at low Reynolds Numbers (Re→0) under different constant hydraulic heads. Water 11.

Whitaker, S., 1986. Flow in porous media I: a theoretical derivation of Darcy's law. Transp. Porous Media 1, 3–25.

WHO, 2019. Guidelines for Indoor Air Quality: Selected Pollutants. European Centre for Environment and Health - Regional Office for Europe, p. 484 Copenhagen, Denmark.

Wilkening, M., 1990. Radon in the Environment.

World Health Organization, 2009. WHO Handbook on Indoor Radon. A Public Health Perspective.

Yarmoshenko, I.V., Onishchenko, A.D., Malinovsky, G.P., Vasilyev, A.V., Zhukovsky, M.V., 2022. MODELING and justification of indoor radon prevention and remediation measures in multi-storey apartment buildings. Results Eng. 16.

Youngquist, G.R., 2002. Symposium on flow through porous media diffusion and flow of gases in porous solids. Industrial & Engineering Chemistry 62, 52–63.

Yu, K.N., 1993. The effects of typical covering materials on the radon exhalation rate from concrete surfaces. Radiat. Prot. Dosim. 48, 367–370.